Four-wave mixing in wavelength–division-multiplexed soliton systems: ideal fibers

M. J. Ablowitz and G. Biondini*

Department of Applied Mathematics, University of Colorado at Boulder, Boulder, Colorado 80309-0526

S. Chakravarty

School of Mathematics, University of New South Wales, Sydney 2052, Australia

R. B. Jenkins and J. R. Sauer

Optoelectronic Computing Systems Center, University of Colorado at Boulder, Boulder, Colorado 80309-0525

Received May 31, 1996; revised manuscript received October 24, 1996

Analytic expressions for four-wave-mixing terms in an ideal, lossless wavelength–division-multiplexed soliton system are derived with an asymptotic expansion of the N-soliton solution of the nonlinear Schrödinger equation. The four-wave contributions are shown to grow from a vanishing background and then to decay. Their importance becomes evident in real, nonideal fibers, where they grow by an order of magnitude and equilibrate to a stable value as an effect of periodic amplification. © 1997 Optical Society of America
[S0740-3224(97)02007-9]

1. INTRODUCTION

The study of soliton communication systems has been marked by a number of important theoretical and technological advances. For example, it is now well known that the effects of amplifier noise, known as Gordon–Haus jitter,[1] can severely limit the transmission rate. This problem has been overcome by the recognition that sliding filters reduce the debilitating effects of noise.[2–4] Wavelength–division-multiplexed (WDM) soliton systems offer the potential for significant increases in data-transmission rates over that of single-channel soliton systems. The difficulties involving WDM solitons are less clear mainly because researchers have not yet clarified all of the potential problems. In an earlier work we discussed one problem: namely, timing jitter caused by multisoliton collisions.[5,6] This is an effect that is similar, in spirit, to that of Gordon–Haus jitter, although it is not caused by amplifier noise; rather it is due to nonuniform soliton interactions because of the presence of amplifiers.

In two recent letters,[7,8] a new and potentially serious problem of WDM systems was discussed: namely, the fact that soliton collisions in the presence of damping and amplification produce significant four-wave interactions. In Ref. 8 we analyzed damping and amplification in detail and presented an analytical and numerical treatment that explains the resonant growth and saturation of the four-wave contributions. In this work we give a comprehensive analytical description of four-wave mixing in ideal fibers, thus providing a useful framework in the study of the more realistic damped-amplifier situation.

2. FOUR-WAVE MIXING FOR THE NONLINEAR SCHRÖDINGER EQUATION

We begin this work by recalling essential formulas.[9] It is well known (see, e.g., Ref. 10) that quasi-monocromatic light propagation in an ideal, Kerr-type, single-transverse-mode optical fiber is described by the nonlinear Schrödinger (NLS) equation

$$iq_z + \tfrac{1}{2}q_{tt} + |q|^2 q = 0, \tag{1}$$

where q is the slowly varying complex envelope of the electric field, while z and t, respectively, are the propagation distance and the retarded time, expressed in the usual nondimensional units.

The N-soliton solution of the NLS can be expressed as a sum over the elements of an $N \times N$ matrix:

$$q(z, t) = \sum_{j,k=1}^{N} (Q^{-1})_{jk}, \tag{2}$$

where the elements of Q are given by

$$Q_{jk} = \frac{\exp(-i\chi_j - S_j) + \exp(-i\chi_k + S_k)}{A_j + A_k + i(\Omega_j - \Omega_k)} \tag{3}$$

and the phases $S_j(z, t)$, $\chi_j(z, t)$ are

$$S_j(z, t) = A_j(t - T_j - \Omega_j z), \tag{4}$$

$$\chi_j(z, t) = \Omega_j t - \tfrac{1}{2}(\Omega_j^2 - A_j^2)z + \phi_j. \tag{5}$$

The solution is specified by $4N$ parameters: A_j, Ω_j, T_j, and ϕ_j, which play the roles of amplitudes, frequen-

 © 1997 Optical Society of America

cies, displacements, and global phases, respectively. It is worth remarking that the quantities $\lambda_j = 1/2(\Omega_j + iA_j)$ are the conserved discrete eigenvalues of the scattering problem associated with the NLS equation (see Ref. 11). Unfortunately, this exact solution is rather complicated, even in the case of $N = 2$. However, in the limit of widely separated frequency channels, which is a case of physical importance, this solution simplifies, and significant information can be obtained.

In the limit of large frequency separations, $|\Omega_j - \Omega_k| \gg 1$ for $j \neq k$ with $A_j \sim O(1)$, it is convenient to introduce the small parameter $0 < \epsilon \ll 1$, defined by

$$\epsilon = \max_{\substack{j,k=1,\ldots,N \\ k\neq j}} |(A_j + A_k)/(\Omega_j - \Omega_k)| \tag{6}$$

[note the denominator of Eq. (3)]. We decompose Q as $Q = D + M$, where D and M are the diagonal and the off diagonal parts, respectively; i.e., $D_{kk} = \cosh S_k \times \exp(-i\chi_k)/A_k$ and $M_{jk} = Q_{jk}$, where $j \neq k$, $j, k = 1, \ldots, N$. Thus $Q^{-1} = (D + M)^{-1} = (I - P + P^2 + \ldots)D^{-1}$, where $P = D^{-1}M$; hence the matrix norm $\|P^n\|$ is $O(\epsilon^n)$. In this way an asymptotic expansion for q is obtained:

$$q(z, t) = q^{(0)}(z, t) + q^{(1)}(z, t) + q^{(2)}(z, t) + \ldots, \tag{7}$$

where $q^{(n)} \sim O(\epsilon^n)$. The first term of the asymptotic series is given by D^{-1} and is simply the superposition of N one-soliton solutions corresponding to the different frequency channels:

$$q^{(0)}(z, t) = \sum_{j=1}^{N} q_j(z, t) \equiv \sum_{j=1}^{N} A_j \exp(i\chi_j)\operatorname{sech} S_j. \tag{8}$$

Each channel is located in the vicinity of the space–time points satisfying the equation $S_j = 0$, i.e., $t = T_j + \Omega_j z$. The frequency spectrum of the corresponding solution consists of N localized contributions, which are peaked around the channel frequencies Ω_j. Because we are considering the limit of widely separated frequency channels, the pulses in frequency space remain well separated even when the solitons interact in physical space. Defining the Fourier transform,

$$\hat{q}(z, \omega) \equiv \mathscr{F}_\omega[q(z, t)] = \int_{-\infty}^{+\infty} \mathrm{d}t \, \exp(-i\omega t) q(z, t), \tag{9}$$

we have

$$\hat{q}_j(z, \omega) \equiv \frac{\pi}{A_j} \exp(i\theta_j)\operatorname{sech}\left[\frac{\pi}{2A_j}(\omega - \Omega_j)\right], \tag{10}$$

where

$$\theta_j(z, \omega) = 1/2(\Omega_j^2 + A_j^2)z - \Omega_j\omega z - T_j(\omega - \Omega_j) + \phi_j. \tag{11}$$

As an example, we show in Fig. 1 a simultaneous three-soliton collision; Fig. 2 displays the corresponding frequency spectrum.

The next contribution in the asymptotic expansion comes from the product $D^{-1}MD^{-1}$, which generates $O(\epsilon)$ and $O(\epsilon^2)$ terms:

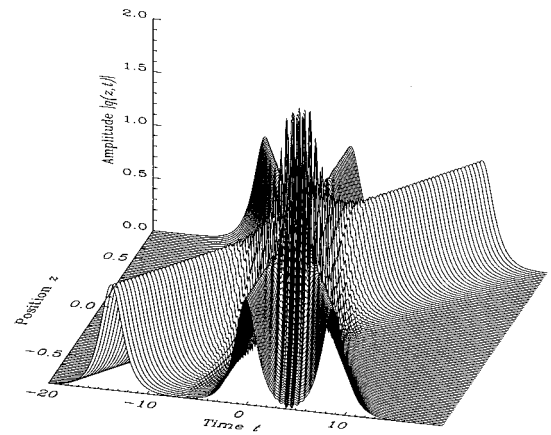

Fig. 1. Simultaneous, three-soliton collision: $A_1 = A_2 = A_3 = 1$, $\Omega_1 = -11$, $\Omega_2 = 0$, $\Omega_3 = 17$, and $T_1 = T_2 = T_3 = 0$.

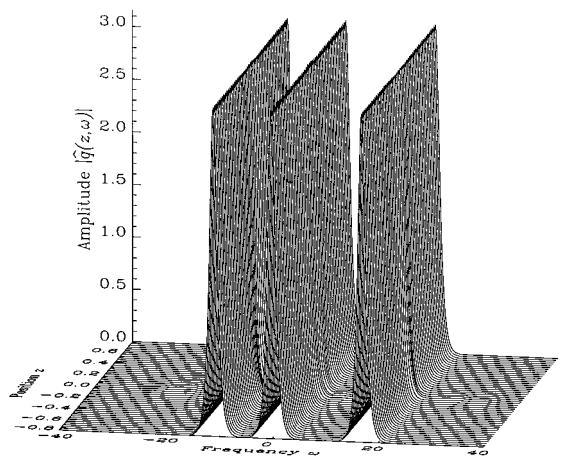

Fig. 2. Fourier spectrum relative to the collision shown in Fig. 1.

$$\begin{aligned} D^{-1}MD^{-1} &= \sum_{\substack{j,k=1 \\ k\neq j}}^{N} A_jA_k \exp[i(\chi_j + \chi_k)]\operatorname{sech} S_j \operatorname{sech} S_k \\ &\quad \times \frac{\exp(-i\chi_j - S_j) + \exp(-i\chi_k + S_k)}{A_j + A_k + i(\Omega_j - \Omega_k)} \\ &\approx i\sum_{\substack{j,k=1 \\ k\neq j}}^{N} \frac{1}{\Omega_j - \Omega_k} q_jq_k[\exp(-i\chi_j)\sinh S_j \\ &\quad - \exp(-i\chi_k)\sinh S_k] \\ &\quad + \sum_{\substack{j,k=1 \\ k\neq j}}^{N} \frac{A_j + A_k}{(\Omega_k - \Omega_j)^2} q_jq_k[\exp(-i\chi_j)\cosh S_j \\ &\quad + \exp(-i\chi_k)\cosh S_k]. \end{aligned} \tag{12}$$

After a symmetrization of indices in the matrix products, the $O(\epsilon)$ contribution can be written as

$$q^{(1)}(z, t) = 2i\sum_{\substack{j,k=1 \\ k\neq j}}^{N} \frac{A_k}{\Omega_j - \Omega_k} q_j \tanh S_k. \tag{13}$$

These terms describe the permanent phase shift that solitons experience during mutual collisions. These perma-

nent phase shifts correspond to the temporary frequency shift of the soliton carrier frequency. The frequency shift is more clearly seen by taking the Fourier transform. In the appendix we show that

$$\int_{-\infty}^{+\infty} \mathrm{d}t\ \exp(-i\omega t)\operatorname{sech} t\ \tanh(t+\Delta) \equiv \pi\ \operatorname{sech}(\tfrac{1}{2}\pi\omega)\ \frac{\cosh\Delta - \exp(i\Delta\omega)}{\sinh\Delta}. \quad (14)$$

Using Eq. (14), with $A_j = 1, j = 1, \ldots, N$, we find

$$\hat{q}^{(1)}(z,\omega) = 2\pi i\ \exp(-i\theta_j)\sum_{\substack{j,k=1\\k\neq j}}^{N} \frac{1}{\Omega_j - \Omega_k} \times \operatorname{sech}[\tfrac{1}{2}\pi(\omega - \Omega_j)] \times \frac{\cosh\delta_{jk} - \exp[i\delta_{jk}(\omega - \Omega_j)]}{\sinh\delta_{jk}}, \quad (15)$$

where

$$\delta_{jk}(z) \equiv S_k - S_j = (\Omega_j - \Omega_k)z + T_j - T_k \quad (16)$$

is a measure of the temporal separation of solitons j and k. That is, $\delta_{jk} = 0$ when soliton j and k interact in the fiber. The effect of these terms on the carrier frequency of the solitons was analyzed in detail in Ref. 9.

Contributions $O(\epsilon^2)$ are calculated in a similar way. They arise from the remaining part of $D^{-1}MD^{-1}$ and from $D^{-1}MD^{-1}MD^{-1}$. They are

$$q^{(2)}(z,t) = 2\sum_{\substack{j,k=1\\k\neq j}}^{N} A_k \frac{A_k + A_j}{(\Omega_k - \Omega_j)^2} q_j + \sum_{\substack{j,k,l=1\\k,l\neq j}}^{N} \frac{A_j A_k A_l}{(\Omega_l - \Omega_j)(\Omega_k - \Omega_j)} \operatorname{sech} S_k \times \operatorname{sech} S_l \operatorname{sech} S_j \times \{\exp(i\chi_j)\cosh\Delta_{kl}^{-} + \exp(i\chi_k)\cosh\Delta_{kj}^{+} + \exp(i\chi_l)\cosh\Delta_{lj}^{+} + \exp[i(\chi_k + \chi_l - \chi_j)]\}, \quad (17)$$

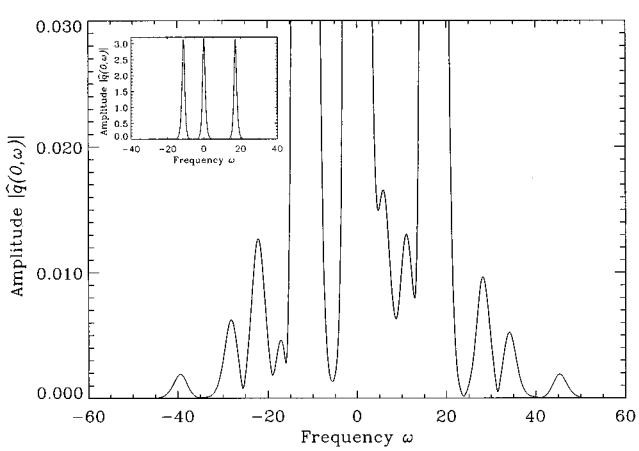

Fig. 3. Nine four-wave frequencies generated during the collision shown in Fig. 1. The inset shows the location of the soliton contributions.

where $\Delta_{kj}^{\pm} = S_k \pm S_j$. It is important to note that all the terms in Eq. (17) are localized in the Fourier domain, and they are all centered around the frequency of the individual soliton channels, *except* for the term corresponding to the last exponential, i.e., $\exp[i(\chi_k + \chi_l - \chi_j)]$. This last term, which we denote q_{FWM}, corresponds to the four-wave interactions of the solitons. It represents contributions peaked around $N^2(N-1)/2$ well-defined frequencies. As an example, Fig. 3 shows the nine four-wave-mixing frequencies that are generated during the collision shown in Figs. 1 and 2.

In the following section we investigate the main features of four-wave interactions in ideal fibers by applying the above formulas in a number of representative situations.

3. FOUR-WAVE MIXING IN IDEAL FIBERS

As a special and physically relevant situation we take $A_j = 1$, $\Omega_k - \Omega_j = (k-j)\Omega$, $k, j = 1, \ldots, N$. Here $\epsilon = 2/\Omega$ and the four-wave contribution is given by

$$q_{\mathrm{FWM}}(z,t) = \tfrac{1}{4}\epsilon^2 \sum_{\substack{j,k,l=1\\k,l\neq j}}^{N} \frac{1}{(k-j)(l-j)} \times \exp[i(\chi_k + \chi_l - \chi_j)]\operatorname{sech} S_k \times \operatorname{sech} S_l \operatorname{sech} S_j, \quad (18)$$

where now $S_j = t - T_j - \Omega_j z$ and $\chi_j = \Omega_j t - \tfrac{1}{2}(\Omega_j^2 - 1)z + \phi_j$. We note that, since the coefficient of $\exp[i(\chi_k + \chi_l - \chi_j)]$ contains a product of three hyperbolic secants, the four-wave-mixing terms are nonnegligible only during soliton collisions when the arguments S_k, S_l, and S_j coincide. Hence from Eq. (18) we see that the four-wave terms grow from a vanishing background, become nonnegligible [i.e., $O(\epsilon^2)$], and then decay back to zero.

Let us be more concrete. We consider the case in which all the solitons collide, say, at $z = 0$ (maximal interaction); i.e., consider the case $T_j = 0, j = 1, \ldots, N$. We also neglect the unimportant relative phases and set $\phi_j = 0$, $j = 1, \ldots, N$. The four-wave contribution at $z = 0$ then is

$$q_{\mathrm{FWM}}(0,t) = \tfrac{1}{4}\epsilon^2 \sum_{\substack{j,k,l=1\\k,l\neq j}}^{N} \frac{1}{(k-j)(l-j)} \times \exp[i(\Omega_k + \Omega_l - \Omega_j)t]\operatorname{sech}^3 t. \quad (19)$$

In the appendix we evaluate the integral (which we will use later as well)

$$\int_{-\infty}^{+\infty} \mathrm{d}t\ \exp(-i\omega t)\operatorname{sech}^2 t\ \operatorname{sech}(t+\Delta) \equiv \pi\ \operatorname{sech}(\tfrac{1}{2}\pi\omega) I(\Delta,\omega), \quad (20)$$

where

$$I(\Delta,\omega) = [\cosh\Delta + i\omega\sinh\Delta - \exp(i\omega\Delta)]/\sinh^2\Delta. \quad (21)$$

Using this result, and noting that $I(0,\omega) = \tfrac{1}{2}(1 + \omega^2)$, we obtain

$$\hat{q}_{\mathrm{FWM}}(0, \omega) = {}^{1}\!/_{8}\pi\epsilon^2 \sum_{\substack{j,k,l=1 \\ k,l\neq j}}^{N} \frac{1}{(k-j)(l-j)} \times \operatorname{sech}[{}^{1}\!/_{2}\pi(\omega - \Omega_{klj})] \times [1 + (\omega - \Omega_{klj})^2], \tag{22}$$

where $\Omega_{klj} \equiv \Omega_k + \Omega_l - \Omega_j$, $k, l \neq j$. Equation (22) represents contributions peaked around the $N^2(N-1)/2$ well-defined frequencies Ω_{klj}.

Equation (22) was derived from the assumption that all the solitons interact at the same time. In general, a simultaneous multisoliton interaction is an exceptional (nongeneric) case, as opposed to the case of nonsimultaneous two-soliton collisions. Nevertheless, an analogous result holds in this more general case. Specifically, if M solitons (with $M \leqslant N$) interact at a given point, Eq. (22) remains valid provided that the values of j, k, l are suitably restricted to the subset of the values corresponding to the solitons that are interacting. That is, at each fixed location z the only nonnegligible terms in Eq. (18) are those corresponding to solitons that are interacting, i.e., with overlapping phases S_k, S_l, and S_j, at that particular time. In what follows we will further elucidate the situation with some examples.

Consider a nonsimultaneous three-soliton collision, with $A_j = 1$, $j = 1, 2, 3$, and $\Omega_1 = -10$, $\Omega_2 = 0$, $\Omega_3 = 10$, so that $\Omega = \Omega_3 = 10$, and $\epsilon = 0.2$. Figure 4 shows the collision in physical space, whereas Fig. 5 depicts the corresponding frequency domain. The four-wave components are barely visible in Fig. 5 as small humps alongside the soliton channels during the collisions. Since in this case the interaction is pairwise, only two four-wave-mixing terms are generated during each collision. For example, during the collision between the first two channels, two four-wave-mixing terms are generated at frequencies $\Omega_{112} = 2\Omega_1 - \Omega_2 = -20$ and $\Omega_{221} = 2\Omega_2 - \Omega_1 = 10$. The component located at $\omega = \Omega_{112}$ is clearly visible in Fig. 5. We note that the component located at $\omega = \Omega_{221}$ is obscured by the third soliton, which is located at the same frequency. However, we can see that the inverse Fourier transform of the frequency region around Ω_3, which is evaluated (numerically) during the collision between solitons 1 and 2, contains both the third soliton *and* a small four-wave component. This four-wave component is located in physical space at the collision point of solitons 1 and 2, as Fig. 6 shows. The inset in Fig. 6 compares this four-wave component with the $\operatorname{sech}^3 t$ profile predicted by Eq. (19); both magnitude and shape match the predictions quite well.

The same choice of parameters can be used to illustrate another interesting feature of four-wave interactions; namely, that during nonsimultaneous collisions the four-wave-mixing term can have a dramatic effect on the frequency range of the solitons that are not participating in the collision. In the specific case we are considering, the frequency range in question is that of soliton 3. During the collision of solitons 1 and 2, which is located at $z_{12} \equiv (T_1 - T_2)/\Omega = -1$, the only significant contributions to the frequency amplitude in the neighborhood of Ω_3 are the soliton component and the four-wave-mixing term,

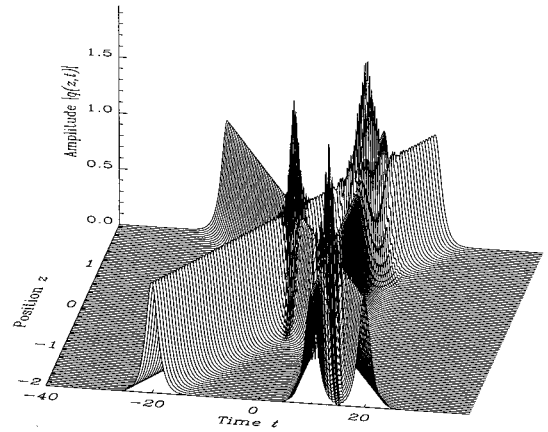

Fig. 4. Nonsimultaneous three-soliton collision: $A_1 = A_2 = A_3 = 1$, $\Omega_1 = -10$, $\Omega_2 = 0$, $\Omega_3 = 10$, $T_1 = 0$, $T_2 = 10$, and $T_3 = 0$.

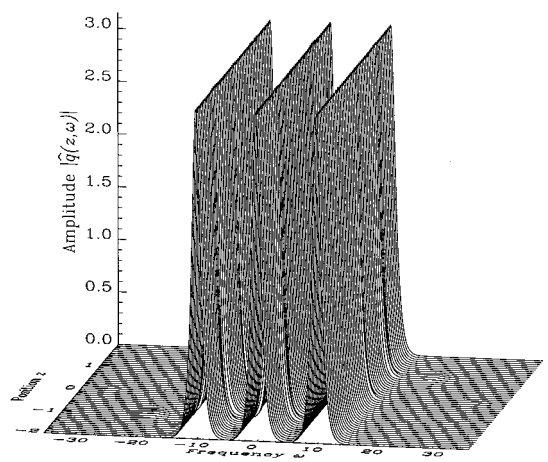

Fig. 5. Fourier spectrum relative to the collision shown in Fig. 1.

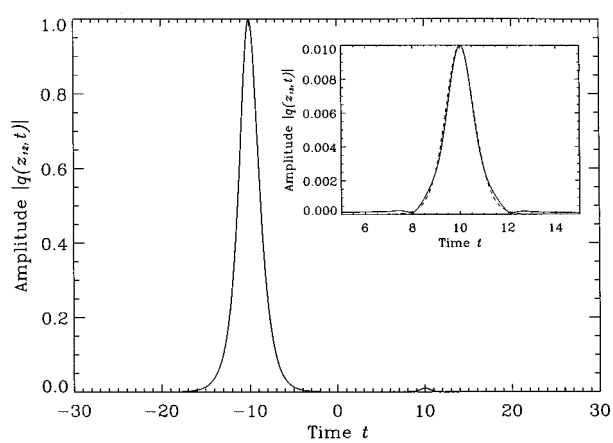

Fig. 6. Inverse transform of the frequency components around Ω_3 during the 1 and 2 collision of Fig. 4. The inset shows a comparison between the FWM component as determined numerically (solid curve) and analytically (dashed curve).

which are, respectively, of $O(1)$ and $O(\epsilon^2)$. The terms $O(\epsilon)$ are exponentially small in the neighborhood of Ω_3 and can therefore be neglected because the third soliton is spatially separated from the first two [cf Eq. (15); see also Ref. 9]. Using the integral defined in Eq. (21), we have

$I(\Delta, \omega - \Omega) \simeq \frac{1}{2}\,\mathrm{sech}^2(\frac{1}{2}\Delta)$ around $\omega = \Omega$. Thus in the neighborhood of $\omega \simeq \Omega_3$ and $z \simeq z_{12}$ the frequency spectrum of the solution is

$$\hat{q}(z, \omega) \simeq \pi\,\mathrm{sech}[\tfrac{1}{2}\pi(\omega - \Omega)] \times \{\exp(i\theta_3) + \tfrac{1}{8}\epsilon^2 \times \exp(i\theta_{221})\mathrm{sech}^2[\tfrac{1}{2}\delta_{21}(z)]\}, \tag{23}$$

where $\delta_{jk}(z) = S_k - S_j = (\Omega_j - \Omega_k)z + T_j - T_k$ is defined in Eq. (16), $\theta_3 = \frac{1}{2}(\Omega^2 + 1)z - \Omega\omega z - T_3(\omega - \Omega)$ is defined in Eq. (11), and $\theta_{221} \equiv \frac{1}{2}(\Omega^2 + 1)z - T_2(\omega - \Omega)$. The location of the maximum of $|\hat{q}|$ clearly depends on the phase difference $\theta_{221} - \theta_3$. Explicitly,

$$|\hat{q}(z, \omega)| \simeq \pi\,\mathrm{sech}[\tfrac{1}{2}\pi(\omega - \Omega)] \times \{1 + \tfrac{1}{8}\epsilon^2\,\mathrm{sech}^2[\tfrac{1}{2}\delta_{21}(z)] \times \cos[\Omega^2 z + \delta_{32}(z)(\omega - \Omega)]\}, \tag{24}$$

where $\sqrt{1 + O(\epsilon^2)} \simeq 1 + \frac{1}{2}O(\epsilon^2)$ is used. Taking $\mathrm{d}|\hat{q}|/\mathrm{d}\omega$ and looking for its zeros, we find the following transcendental equation, which determines the frequency at maximum modulus at $z \simeq z_{12}$:

$$\omega = \Omega - \tfrac{1}{2}(\epsilon/\pi)^2\delta_{32}(z)\mathrm{sech}^2[\tfrac{1}{2}\delta_{21}(z)] \times \sin[\Omega^2 z + \delta_{32}(z)(\omega - \Omega)], \tag{25}$$

where the approximation $\tanh(\omega - \Omega) \simeq \omega - \Omega$ for $\omega \simeq \Omega$ is used. The maximum of $|\hat{q}|$ oscillates around $\omega = \Omega$ as a function of z with frequency $\Omega^2 \sim O(\epsilon^{-2})$. Observe that the actual amplitude of the oscillations is *not* $O(\epsilon^2)$, because $\delta_{32}(z) \simeq \Omega z \sim O(\epsilon^{-1})$. That is, the resulting amplitude is $\frac{1}{2}(\epsilon/\pi)^2\delta_{32}(z)\,\mathrm{sech}^2[\frac{1}{2}\delta_{21}(z)] \sim O(\epsilon)$. Also, the amplitude of the oscillations decays exponentially as solitons 1 and 2 separate after the collision. The fast oscillations of the maximum in numerical simulations of the collision can be observed in Fig. 7 (see also Ref. 5). The amplitude and the frequency of the oscillations perfectly match the above predictions based on Eq. (25).

Note that, contrary to the $O(\epsilon)$ frequency shift that solitons 1 and 2 undergo during interaction, these oscillations do not represent a change in the actual frequency of the solitons. In fact, the frequency modification predicted by Eq. (25) is caused by the interference between two components, namely, the soliton and the four-wave-mixing term. These two contributions are simultaneously present in the same frequency region, but they actually correspond to terms that are separated in physical space (as seen in Figs. 5 and 6).

It should also be remarked that in the case of simultaneous collisions, there is no corresponding high-frequency oscillation, since in this case, all the $\delta_{jk}(z)$ vanish simultaneously during the interaction, and the corresponding term $\delta_{32}(z)$ in Eq. (25) is zero. There is, however, the $O(\epsilon)$ correction to the frequency of the interacting solitons, as a result of the terms present in $q^{(1)}$ [cf Eq. (15); see also Refs. 9 and 12]. This fact is illustrated in Fig. 8, where the displacements T_j of the solitons are chosen in such a way that the collision is simultaneous.

Again we emphasize that in the ideal case, the four-wave-mixing energy is reabsorbed into the soliton components after the collision process is completed. However, this is not the case when damping and amplification are introduced in the system. As an example, we show in Fig. 9 a numerical simulation of a nonsimultaneous three-soliton collision with damping and amplification, whereas Fig. 10 displays the corresponding frequency spectrum. It is evident that the amplification process induces instability and growth of the four-wave-mixing terms, which have an amplitude that becomes many times larger than in the unperturbed case and saturates after the collision is completed. This is unlike the ideal case, in which the amplitudes grow and then return to zero. In both the ideal and the amplified cases, some of the four-wave frequencies coincide with the soliton carrier frequencies. Hence we observe the same interference phenomenon described before. However, because of the resonant growth of the four-wave-mixing term and their stable, nonzero

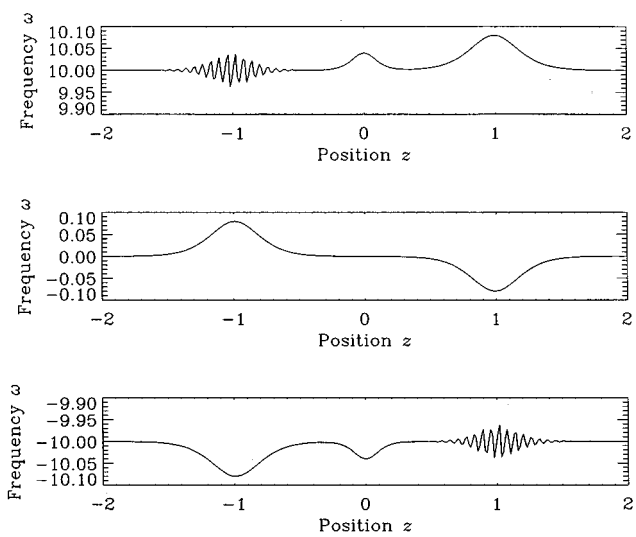

Fig. 7. Location of the maxima of $|\hat{q}|$ for the collision process shown in Fig. 4. The $O(\epsilon)$ frequency shifts of the colliding solitons are visible, together with the corresponding frequency oscillations induced in the third channel.

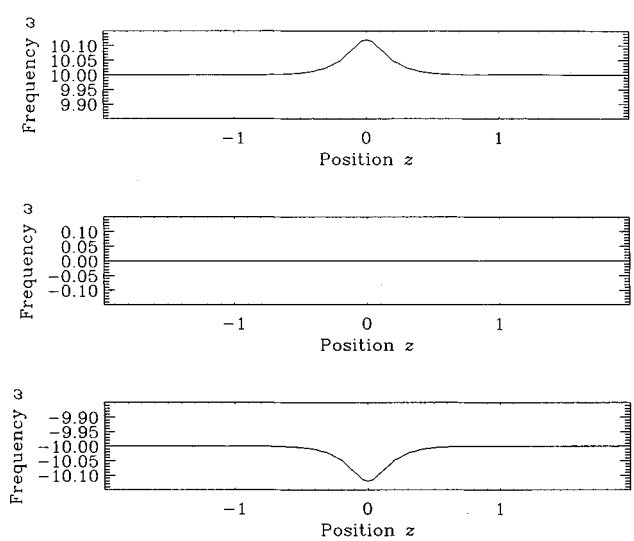

Fig. 8. Same as Fig. 7, but for a simultaneous collision, i.e., $T_1 = T_2 = T_3 = 0$.

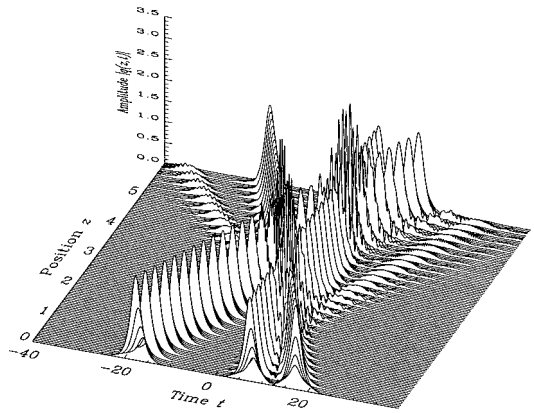

Fig. 9. Nonsimultaneous, three-soliton collision in the presence of damping and periodic amplification: $A_1 = A_2 = A_3 = 1$, $\Omega_1 = -6$, $\Omega_2 = 0$, $\Omega_3 = 6$, $T_1 = 17.5$, $T_2 = 7.5$, and $T_3 = -17.5$. The loss coefficient and the amplifier distance, expressed in nondimensional units, are $\Gamma = 10$ and $z_a = 0.2$, respectively.

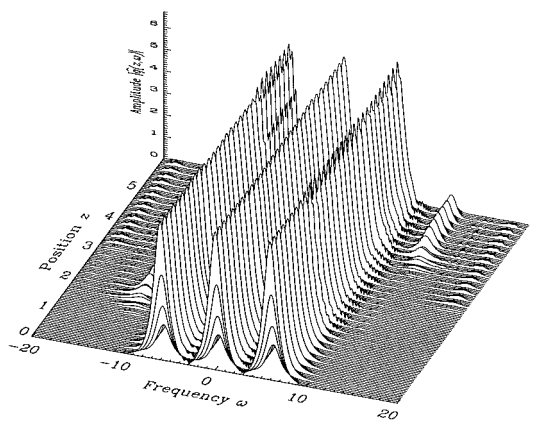

Fig. 10. Frequency spectrum relative to the collision shown in Fig. 9.

asymptotic value, in this case we observe much larger perturbations in the frequency channels of the solitons. This effect has potentially serious implications on the overall properties of the system and could significantly increase the error rates in long-distance communications. An analytical and numerical study of the effects of damping and amplification on four-wave interactions can be found in Ref. 8.

APPENDIX A

Below, we calculate the following Fourier transforms:

$$\mathscr{F}_\alpha[\operatorname{sech}\zeta\tanh(\zeta+\Delta)],\quad \mathscr{F}_\alpha[\operatorname{sech}^2\zeta\operatorname{sech}(\zeta+\Delta)], \tag{26}$$

where

$$\mathscr{F}_\alpha[f(\zeta)] \equiv \int_{-\infty}^{+\infty} d\zeta\,\exp(-i\alpha\zeta)f(\zeta). \tag{27}$$

In both cases, i.e., when $f(\zeta) = \operatorname{sech}\zeta\tanh(\zeta+\Delta)$ and when $f(\zeta) = \operatorname{sech}^2\zeta\operatorname{sech}(\zeta+\Delta)$, the computation is performed by closing the integration contour in the complex ζ plane, employing the periodicity of the hyperbolic functions along the direction of the imaginary axis. We use the identities $\sinh(x+iy) = \sinh x\cos y + i\cosh x\sin y$ and $\cosh(x+iy) = \cosh x\cos y + i\sinh x\sin y$, and we take a rectangular contour with vertices at points $\zeta = \pm R$, $\pm R + \pi i$. In both cases the integrals over the short sides (i.e., from $\pm R$ to $\pm R + \pi i$) vanish in the limit $R \to \infty$. The singularities inside the contour are located at $\zeta = {}^1\!/_2\pi i$ and $\zeta = -\Delta + {}^1\!/_2\pi i$. Thus in both cases,

$$[1+\exp(\pi\alpha)]\int_{-\infty}^{+\infty} d\zeta\,\exp(-i\alpha\zeta)f(\zeta) = 2\pi i\{\operatorname{Res}[\exp(-i\alpha\zeta)f(\zeta)]_{\zeta={}^1\!/_2\pi i} + \operatorname{Res}[\exp(-i\alpha\zeta)f(\zeta)]_{\zeta=-\Delta+{}^1\!/_2\pi i}\}. \tag{28}$$

For the first transform the singularities are simple poles. The residues are readily computed; they are

$$\operatorname{Res}[\exp(-i\alpha\zeta)\operatorname{sech}\zeta\tanh(\zeta+\Delta)]_{\zeta={}^1\!/_2\pi i} = -i\exp({}^1\!/_2\pi\alpha)\tanh\Delta, \tag{29}$$

$$\operatorname{Res}[\exp(-i\alpha\zeta)\operatorname{sech}\zeta\tanh(\zeta+\Delta)]_{\zeta=-\Delta+{}^1\!/_2\pi i} = i\exp({}^1\!/_2\pi\alpha + i\alpha\Delta)\operatorname{csch}\Delta. \tag{30}$$

Hence

$$\mathscr{F}_\alpha[\operatorname{sech}\zeta\tanh(\zeta+\Delta)] = \pi\operatorname{sech}({}^1\!/_2\pi\alpha)\frac{\cosh\Delta - \exp(i\alpha\Delta)}{\sinh\Delta}. \tag{31}$$

The second transform is computed in a similar way. Now the singularities are a double pole at $\zeta = {}^1\!/_2\pi i$ and a simple pole at $\zeta = \Delta + {}^1\!/_2\pi i$. The residues are

$$\operatorname{Res}[\exp(-i\alpha\zeta)\operatorname{sech}^2\zeta\operatorname{sech}(\zeta+\Delta)]_{\zeta={}^1\!/_2\pi i} = -i\frac{\exp({}^1\!/_2\pi\alpha)}{\sinh^2\Delta}(\cosh\Delta + i\alpha\sinh\Delta), \tag{32}$$

$$\operatorname{Res}[\exp(-i\alpha\zeta)\operatorname{sech}^2\zeta\operatorname{sech}(\zeta+\Delta)]_{\zeta=-\Delta+{}^1\!/_2\pi i} = i\frac{\exp({}^1\!/_2\pi\alpha)}{\sinh^2\Delta}\exp(i\alpha\Delta). \tag{33}$$

Hence

$$\mathscr{F}_\alpha[\operatorname{sech}^2\zeta\operatorname{sech}(\zeta+\Delta)] = \pi\operatorname{sech}({}^1\!/_2\pi\alpha)\times\frac{\cosh\Delta + i\alpha\sinh\Delta - \exp(i\alpha\Delta)}{\sinh^2\Delta}. \tag{34}$$

ACKNOWLEDGMENTS

This effort was sponsored by the U.S. Air Force Office of Scientific Research, Air Force Materials Command, under grants F49620-94-0120 and F49620-94-0167. The U.S. Government is authorized to reproduce and distribute reprints for governmental purposes notwithstanding any copyright notation thereon. The views and conclusions contained herein are those of the authors and should not be interpreted as necessarily representing the official

policies or endorsements, either expressed or implied, of the U.S. Air Force Office of Scientific Research or the U.S. Government.

*Permanent address: Dipartimento di Fisica, Università di Perugia and Istituto Nazionale di Fisica Nucleare, Sezione di Perugia, 06112 Perugia, Italy

REFERENCES

1. J. P. Gordon and H. A. Haus, Opt. Lett. **11**, 665 (1986).
2. A. Mecozzi, J. D. Moores, H. A. Haus, and Y. Lai, Opt. Lett. **16**, 1841 (1991).
3. Y. Kodama and A. Hasegawa, Opt. Lett. **17**, 31 (1992).
4. L. F. Mollenauer, J. P. Gordon, and S. G. Evangelides, Opt. Lett. **17**, 1575 (1992).
5. R. B. Jenkins, Ph.D. dissertation (University of Colorado, Boulder, Colorado, 1995).
6. R. B. Jenkins, J. R. Sauer, S. Chakravarty, and M. J. Ablowitz, Opt. Lett. **20**, 1964 (1995).
7. P. V. Mamyshev and L. F. Mollenauer, Opt. Lett. **21**, 396 (1996).
8. M. J. Ablowitz, G. Biondini, S. Chakravarty, R. B. Jenkins and J. R. Sauer, Opt. Lett. **21**, 1646 (1996).
9. S. Chakravarty, M. J. Ablowitz, J. R. Sauer, and R. B. Jenkins, Opt. Lett. **20**, 136 (1995).
10. G. P. Agrawal, *Nonlinear Fiber Optics* (Academic, San Diego, 1995).
11. M. J. Ablowitz and H. Segur, *Solitons and the Inverse Scattering Transform* (Society for Industrial and Applied Mathematics, Philadelphia, 1981).
12. L. F. Mollenauer, S. G. Evangelides, and J. P. Gordon, J. Lightwave Technol. **9**, 362 (1991).